IMAGE MOTION IN AIR PHOTOGRAPHY

Duncan E. Macdonald, Optical Research Laboratory, Boston University

DISCUSSIONS at the Eighteenth Annual meeting of the Photogrammetric Society have prompted this review of vibration effects in aerial photography.

It has long been recognized that in-the-air performance of an air camera system will be inferior to the laboratory performance of the same system. For example, extensive studies employing a 24-inch $f/6$ Aero Ektar lens, which in the laboratory revealed some 25 lines/mm., indicated an in-the-air performance of 11.9 lines/mm. in the direction of flight and 11.4 lines/mm. normal to the line of flight. The air photographs used in this particular study were taken from 25,000 feet in an F-5 aircraft. The flight missions were conducted by the Photographic Laboratory at Wright Field and were programmed by the NDRC testing section at M.I.T. The results were obtained from an analysis of 1,245 target images, which was conducted at and reported on by the Mt. Wilson Observatory.[1]

There are many factors that contribute to the image degradation that is observed in flight. These include, among others, haze, image motion, atmospheric turbulence, and a host of unfavorable environmental conditions to which the equipment is subjected. This paper treats only those factors that contribute to this degradation through a physical motion of an image point in the plane of the emulsion surface.

In the past, some misunderstandings have arisen concerning the assignment of direction to resolution. It is noted here that convention dictates that lines whose length parallels the direction of flight measure the ability to separate detail across the line of flight, and, therefore, measure resolution across the line of flight; and, conversely, that lines perpendicular to the flight direction measure resolution in the line of flight.

Translation of the aircraft introduces a constant image velocity tending to degrade the resolution in the flight line, while over-all aircraft motions and the camera-mount vibrations introduce effects that impair definition in all azimuths. These effects can be broken down into pure roll, pitch, and yaw components. In terms of resolution, roll impairs resolution across the line of flight, pitch degrades resolution in the line of flight, and yaw affects resolution normal to any radius vector from the principal point (i.e., tangential resolution).

There are other image motion effects which have been studied and which have been found to be of less importance in terms of the image degradation. These include: vibration imparted by the shutter; vibration of components of the cone, camera, and magazine combination; vibration of the lens elements in their cells and/or the lens in its cone; any of these may act in any azimuth.

Conventionally, we list resolution in and across the line of flight. In practice, the azimuth of best resolution (and poorest) is generally in neither of these directions, for the resultant of the accidental motions may occur in any azimuth, Assume we are given a photographic system which shows a circular blur point and which gives a photographic resolution of R_a (this would be constant for all azimuths). We may say that the diameter, d, of this blur point is proportional to the inverse of the resolution, i.e.,

$$d = K/R_a. \tag{1}$$

In the simplest case, if this image is subject to a uniform linear motion over a distance, T, in the direction $\theta = 0$ during the exposure, the boundary of the minimal blur element may be described by the rotation of the vector $\frac{1}{2}(K/R_a + bT \cos \theta)$ through 2π, where b is a constant. Thus the resolution in any given azimuth, θ, is given by an expression of the form

$$R(\theta) = R_a/K + bR_aT \cos \theta. \tag{2}$$

If one or more components change in rate during the exposure, the distribution of photographic density within the blur point is changed. If one or more components change in sense during the exposure, the simple concept of shape as above is no longer valid. Although both these effects change in sense and rate, are generally present, and bear directly on the visual detection characteristics, they may be considered to be second order effects in so far as the present state of the art is concerned.

In order to gain some insight into the transitory nature of the aerial performance, the Mt. Wilson results were summarized in the form of cumulative frequency curves (Figure 1).[2] Perhaps the most significant point in viewing the

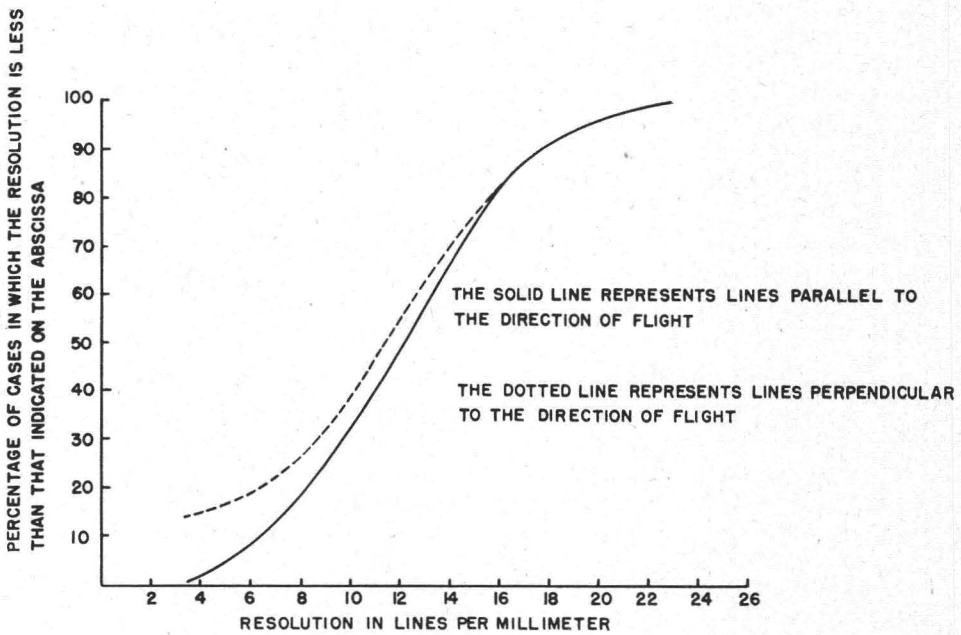

FIG. 1. Combined frequency distribution of resolution.

results of the Mt. Wilson report is that in approximately two per cent of the pictures taken under excellent photographic conditions, the system approximated its laboratory performance in at least one coordinate. This, with the observed wide range in performance, would seem to indicate that the significant factors in limiting resolution on a good photographic day are those which themselves vary widely and can occasionally add up to produce a null effect in a given coordinate.

Certainly, image motion, as caused by or affected by vibration, is this type

of phenomenon, and, therefore, studies of the magnitude of the image deterioration due to vibration are well warranted.

Several methods have been considered in the approach to the analysis of vibration effects. In such a study, it is well to bear in mind that the desired end is the determination of the motion of the image on the film under photographic conditions. It was our feeling that this end was most simply achieved by flights at night with open shutter. In the early flights, the missions were undertaken over neon lights, and later over special Edgerton flash lamps. The periodic flashing of these sources (neon at 120 flashes/sec., the special Edgerton lamps at 60 flashes/sec.) impressed a dotted time scale on the film that could be used for assessing the rates of image excursion.

A considerable amount of valuable vibration data can be obtained by means of a rapid, simple, and inexpensive analysis, whereas more accurate data can be processed by more complex analysis methods. It is important to note that in no case is special ground test equipment necessary.

A possible flight test operation is now described. The filter is removed, the lens set at about $f/6$, the shutter locked open, the loaded magazine mounted on the camera, and the camera then mounted in the aircraft. The film in the focal plane thus serves as a "shutter," protecting the next frame from exposure. Flights that provide an approximate 1:3,000 scale at ground speeds of about 150 mph offer good separation of points for analysis. A flight line is laid out, preferably over a not too well populated area, normal to a street that has several neon signs; the only stringent requirement is, however, that the pass be over some sign or light with a known periodic characteristic. We have considered in this general description the usually encountered frequency of 120 cps. A fresh piece of film is cycled into the focal plane as the aircraft lines up for a straight level pass over the lamps; then, before turning out of the run, a new piece of film is cycled into the focal plane. By this means, the record of the level photographic run is protected from the loops and curls that are recorded in banks and turns of the aircraft. (In such tests made over city lights, the duration of the exposure should be approximately the time it takes the plane to translate the image the length of the frame. Longer times introduce a confusion generated by the appearance of many light trails with no time relationship between them. For example, one trail may start long after an adjacent and parallel trail has been recorded and the first source is well out of the field of view.)

It is apparent that if the flight line is straight and level and without any vibrations, a single lamp will record on the film as a straight line of uniformly spaced dots, and two ground lamps will appear as parallel trails. Roll of the camera and/or its mount, or of the aircraft as a whole, will cause displacement of the trails normal to the direction of forward motion of the aircraft, i.e., introduce a sine wave appearance to the trace on the film. Pitch will cause an alternate compression and expansion of the spacing of the dots but will not affect the direction of the trail. Yaw is most easily seen in terms of the effect on corresponding points in two parallel trails. Assume that a line between two points which were recorded at the same time instant is normal to the direction of forward motion of the plane, i.e., perpendicular to the two parallel trails that these lamps generate. If yawing takes place at some later time on the trail, this line, joining the corresponding time points of the two trails, is shifted from its orientation normal to the trails. It departs from normality by an amount equal to the yaw angle.

In this type of test, exposure is controlled entirely by the aperture of the lens

and the spacing of the points by the scale-ground speed relationship. Inasmuch as lamps which are typical of the type encountered in flying over cities, such as neon signs, are on longer than they are off, the flashes are drawn in long sausage-shaped images. In this case, for detailed analysis, it is easier and more accurate to measure to the center of the spaces between flashes.

The appearance of a single trail (under considerable magnification) is simulated by the dotted line in Figure 2. As it is known that the dots (assuming neon

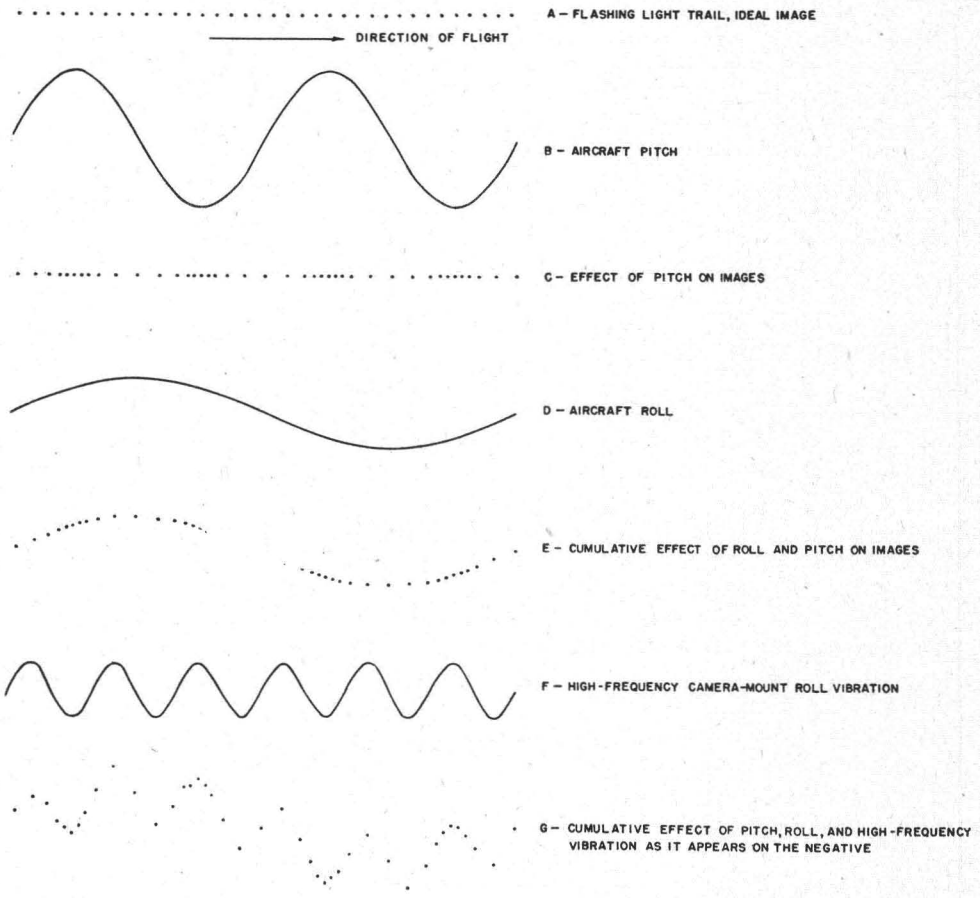

FIG. 2. An exaggerated schematic showing the frequency analysis of a flashing light trail.

lights) are spaced 1/120 second apart in time, frequencies may be determined by counting dots over a few waves. Four common effects are shown in this figure, and, for purposes of illustrating them, they are individually removed from the simulated trail:

a. The over-all aircraft roll: All vibrations of frequency below one cycle per second were assigned to the over-all aircraft roll. There has been no difficulty or apparent departure from realism by this arbitrary assumption, for, in all reciprocating engine aircraft yet tested, the highest frequency of aircraft motions encountered occurred between two and three cycles per second, while the lowest frequency camera-mount vibrations run about eight cycles per second.

b. The camera-mount roll superimposed on the over-all aircraft roll, subject to beat frequencies.
c. Beat frequencies: These effects are apparently due, respectively, to air-frame characteristics and lack of perfect engine synchronization.
d. The camera-mount pitch: This causes a periodic change in point spacings.

From this we see that very simple methods may be employed to gather much information. For example, we can learn much about important vibration components (both frequencies and amplitudes) in a few minutes, using only a simple rule and magnifier. With a rule to measure amplitudes, and by counting dots to determine frequencies, the roll characteristics can be approximated, the beat characteristics determined, and the pitch frequency of the camera-mount system determined. This is enough data to provide considerable insight into comparative performance of different camera-mount-aircraft combinations, as we shall see in more detail later on.

On the basis of the previous work it appears valid to assume that the roll effects are simple harmonic motions. Thus, the amplitude of displacement of the point at any time, t, is given by

$$S = A \sin (2\pi t/T)$$

where A is the measured amplitude and T the measured period of the phenomenon. However, we are more interested in the displacement of the image during an exposure, and thus we are concerned with the image velocity on the film, V, and the total image excursion, W, during the exposure time, Δt. At any given time, t,

$$V = 2\pi A/T \cos (2\pi/T)t,$$

and to a first order approximation

$$W = V/\Delta t,$$

from which we can determine the following:

the maximum image excursion during exposure,

$$W_{\max} = 2\pi A/T(\Delta t); \tag{3}$$

the average image excursion during exposure,

$$W_{\text{ave}} = 4A/T(\Delta t); \tag{4}$$

and the median image excursion during exposure,

$$W_{\text{med}} = 1.414\pi A/T(\Delta t). \tag{5}$$

In terms of degradation, these magnitudes are to be compared with the constant translation of the image, W_T, where

$$W_T = vf/h\Delta t. \tag{6}$$

Here, v is the ground speed, h is the altitude, and f is the focal length. This may most simply be determined from the film; measuring on the film the distance x_n that the image travels while n points are recorded at flashing frequency of g cycles per second, then

$$W_T = gx_n/n(\Delta t). \tag{7}$$

This translational component is constant with the accidental motions superimposed. The recent trend has been toward introduction of image movement compensation (i.m.c.) to treat this predictable factor. The magnitude of this factor may be illustrated by a plot of the form of Figure 3.

In order to establish the use of these simple methods and cognizance of the requisite precautions, it is in order to present a more detailed analysis method. Several such methods have been studied and employed. Although the particular one selected here is the simplest of these, it treats in detail the analysis of the vibration effects of over-all aircraft motions and camera-mount vibrations.

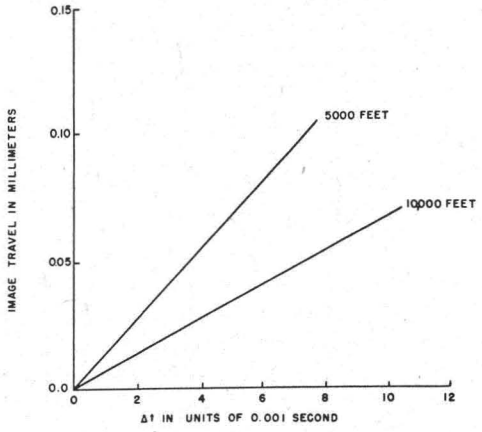

FIG. 3. Image travel due to 300 MPH translation as a function of exposure time for a 6-inch lens.

This method of reduction may be described as a single trail or an (uncorrected) two-trail method of analysis. A major share of the credit for development of the particular analysis form belongs to Miss Lillian R. Elveback and to the analysts in the M.I.T. testing program.

The formal analysis requires comparator determinations of the coordinate positions of the trail points. To undertake this, select a film with two or more neon trails. The direction of flight on the film must first be determined. This may be done by identifying corresponding points on the two trails (by "corresponding" is meant two points that occur at the same instant of time). The identification may be established by observing the trail configurations, marking off corresponding features, and identifying points which by unique correspondence of surrounding configuration, are identified as having occurred at identical times. To connect these two points, a line is then drawn on the film. (This is best done by drawing a knife across the gelatin, which forms a fine marking for measurement purposes.) This line is taken as parallel to the Y axis. A line parallel to the x axis is then drawn, i.e., normal to the first line. This is taken to be the direction of flight. If, at the particular points chosen, the plane happened to be yawing, the average direction of flight over the film might differ from the X axis by a few mils. If the course of flight is obviously not normal to the line connecting the lamps, then it will serve as well to draw in an X axis along that direction which appears to be the direction of flight, as best assessed by observation of the general direction of the trails. The choice of the coordinate system affects only the zero attitude of the plane and camera, and does not affect the results which are of interest to us, for these are to be expressed as rates and are, therefore, unaffected by all but gross errors in the choice of this zero attitude. The origin of the coordinate system is then taken at the approximate center of the negative, the X axis parallel to the flight direction and the Y axis normal to this.

The XY position of the trail points (or spaces between) are measured on a comparator or by some such means. (Automatic measuring devices lend themselves to consideration if any large number of reductions are to be made.)

The philosophy that underlies the method, in all cases, is to determine the ideal coordinates which the points would possess if no vibrations were present and if the flight were level and with uniform translational velocity. Departures of the points from these ideal positions, as observed on the film, are then taken to be a measure of departure from smooth level flight. Velocities are then determined from differences in attitude at successive points. For the first part of this method only a single trail need be completely measured. Three or four points on a second trail (b) should also be measured at each of five or ten well separated areas. These points must be identified with their corresponding points on the (a) trail.

Let the central trail point be the zeroth point, and consider n points on either side of this. Then the average x interval between points of a trail is determined by considering the entire trail which consists of $(2n+1)$ points.

$$\overline{\Delta x_a} = x_a{}^{(n)} - x_a{}^{(-n)}/2n \tag{8}$$

where superscripts refer to the number of the point, and subscripts (a) or (b) refer to trail (a) or (b).

The average y position is given by

$$\overline{y_a} = \sum_{k=-n}^{n} Y_a{}^{(k)}/2n + 1. \tag{9}$$

Due to changes in altitude and the departure of the optical axis from a vertical orientation, the true separation of the two trails D is not constant over the entire trail at the kth point.

$$D^{(k)} = \left| y_a{}^{(k)} \right| + \left| y_b{}^{(k)} \right|.$$

The ideal trails, subscript i, can be determined by first plotting D for several well separated regions on the film against the time (or point number), and this (assumed) linear function applied in the following manner (Figure 3 is the plot of D against time from a typical analysis):[4]

$$\overline{D} = \left| \overline{y_a} \right| + \left| \overline{y_b} \right| = D^{(0)},$$

since the function is regarded as linear.

$$D^{(k)} = kc + \overline{D},$$

where c is the slope of the graph (Figure 3).

Scale change due to changing altitude or non-vertical orientation of the optical axis is then expressed by

$$y_{ai}{}^{(k)}/\overline{y_a} = D^{(k)}/\overline{D} = \Delta x_{ai}{}^{(k)}/\Delta x_a.$$

Thus the ideal y value for any point can be written

$$y_{ai}{}^{(k)} = \overline{y_a} + hk, \tag{10}$$

where

$$h = (\overline{y_a}/\overline{D})c.$$

As

$$x_{ai}^{(k)} = x_{ai}^{(k-1)} + \Delta x_{ai}^{(k)},$$

the ideal x value for any point may be written:

$$x_{ai}^{(k)} = x_{ai}^{(k-1)} + pk + \Delta x_a, \tag{11}$$

where

$$p = (\overline{\Delta x_a}/\overline{D})c,$$

or, as an alternate form,

$$x_{ai}^{(k)} = k[([k+1]/2)p + \overline{\Delta x_a}].$$

Thus the ideal trail may be computed.

Now, set

$$x_{ai}^{(0)} = x_a^{(0)}.$$

Roll, α, of the camera or aircraft produces motion on the film across the direction of flight; pitch, β, produces motion in the direction of flight.

The attitude of the camera at any point, k, can be determined to a first approximation by the following:

$$\sin \alpha_0^{(k)} = \delta y_a^{(k)}/f, \tag{12}$$

and

$$\sin \beta_0^{(k)} = \delta x_a^{(k)}/f, \tag{13}$$

where

$$\delta y_a^{(k)} = y_a^{(k)} - y_{ai}^{(k)}$$

and

$$\delta x_a^{(k)} = x_a^{(k)} - x_{ai}^{(k)}$$

and f is the focal length of the camera.

Angular velocities (the dot notation is used to indicate the time derivative, i.e., $\dot{\alpha} = d\alpha/dt$) can be expressed by the following, since the angles are small:

$$\dot{\alpha}_0^{(k)} = \lambda(\delta y_a^{(k)} - \delta y_a^{(k-1)}), \tag{14}$$

$$\dot{\beta}_0^{(k)} = \lambda(\delta x_a^{(k)} - \delta x_a^{(k-1)}), \tag{15}$$

where $\lambda = 120{,}000/f$ when the frequency of the flashing lamps is 120 cycles/sec. The resulting angular velocities are expressed in mils/sec. If yaw motion is also desired, it becomes necessary to measure completely the second trail on the film. (Past experience, although not with cameras of six-inch and shorter focal length, indicates that yaw has much less effect on image deterioration than does roll and pitch, and might then be reasonably relegated to the role of a second order effect. This is as would be expected with long focal length cameras, for roll and pitch operate with the focal length as the radius, whereas yaw has for its radius the distance from the center of the film to the point of interest. On a nine-by-nine format, fifty per cent of the picture information is inside a 3.6-inch radius.) To determine yaw it is necessary that a time correspondence be established be-

tween the trails and that the zeroth points of trails (a) and (b) coincide in time.

The procedure involved in the two-trail reduction method is similar to the above. $\overline{\Delta x_a}$, $\overline{\Delta x_b}$, $\overline{y_a}$, and $\overline{y_b}$ are determined by equations (3) and (4). Equations (5) and (6) are employed for each trail, and roll and pitch are averaged over the two trails.

$$\sin \alpha_0^{(k)} = \delta y_a^{(k)} + \delta y_b^{(k)}/2f.$$

$$\sin \beta_0^{(k)} = \delta x_a^{(k)} + \delta x_b^{(k)}/2f.$$

Yaw, γ, produces motion normal to any radius drawn from the origin, and for any given yaw angle the displacement on the film is proportional to $(x^2-y^2)^{1/2}$ at that point. The yaw attitude can be determined from the expression

$$\sin \gamma_0^{(k)} = x_a^{(k)} - x_b^{(k)}/D^{(k)}.$$

The velocity expressions for this method are similar to the single trail expressions which can be written simply as:

$$\dot{\alpha}_0 = \alpha^{(k)} - \alpha^{(k-1)}/t,$$

$$\dot{\beta}_0 = \beta^{(k)} - \beta^{(k-1)}/t,$$

and

$$\dot{\gamma}_0 = \gamma^{(k)} - \gamma^{(k-1)}/t = \Delta x_a^{(k)} - \Delta x_b^{(k)}/tD^{(k)},$$

where, in this expression, t is the time between successive points, 1/120 second.

A simple form for handling the analysis is to tabulate in the manner shown on the following.

Point number	Measured x value		
n	x_a	x_{ia}	δx_a
k	$x_a^{(k)}$	$x_i^{(k-1)}+kp+\overline{\Delta x_a}$	$x_a^{(k)}-x_i^{(k)}$

	Measured y value			
β_0	y_a	y_{ia}	δy_a	α_0
$\lambda(\delta x_a^{(k)}-\delta x_a^{(k-1)})$	$y_a^{(k)}$	$\overline{y_a}+kh$	$y_a^{(k)}-y_{ia}^{(k)}$	$\lambda(\delta y_a^{(k)}-\delta y_a^{(k-1)})$
			where $\lambda=120{,}000/f$	

After comparison of analyses, by the above and then by more elaborate methods, it became apparent that the agreement between the results warranted no more effort than that expended in the method as described above. All methods gave identical results across the center of the photographic plate. It is, therefore, apparent that the above method applied to the central portion of the film (portions restricted to a six-inch diameter circle centered on the principal point) gives an adequate analysis of the camera-mount vibration.

Throughout the past work, it has been observed that there is a marked

similarity, both in appearance on the film and in the results derived by the analysis, between the individual frames and between flights employing any given camera-mount combination. This has led us to believe that a study of two or three seconds of a single trail on a single pass will give a good representation of the distribution of image motions due to the vibrations of the camera-mount combination. It should not, however, be taken as sufficient for a detailed analysis but should serve only for a general comparison between camera-mount combinations.

Conversely, the image-motion characteristics introduced by over-all aircraft motion differ from pass to pass, and it seems that the over-all aircraft motions cannot be predicted within any reliable limits until several frames are analyzed.

Figure 4 is a series of contact prints made from several typical vibration trails. The scale in each case is approximately 1:2,500. It is hoped that, by presenting these in this form, it is possible to convey a general feeling for the method, and, by looking at the results that follow, also to convey an "order of magnitude" feeling for the performance.

Plates *A* and *B* depict performance of a center-of-gravity mount, designed by Dr. J. G. Baker of Harvard College Observatory, where two 40-inch cameras are balanced on a 1/16-inch diameter ball bearing. Plate *A* shows the performance during a period when there was little aircraft motion. Plate *B* still shows the characteristic smooth trail in the presence of over-all aircraft motion. This type of mount, designed to illustrate the ultimate in center-of-gravity mounting, has given by far the best anti-vibration characteristic of any mount examined.

Plate *C* shows the performance of a high-compliance spring mount, designed by Dr. J. S. Chandler of the Eastman Kodak Company. On this pass there were no angular aircraft motions. One notices a relatively low-frequency vibration component present which has been forced by the air-frame vibration.

Plates *D* and *E* are taken from passes made with the A-8 and A-11 mounts, respectively. Both of these mounts pass considerable air-frame vibration which is superimposed on varying degrees of aircraft motion.

Plate *F* shows the performance of the prototype A-28 gyro stabilized mount. Here the gyro corrects for the low-frequency aircraft motions, providing for a level camera during flight, but superimposed is the high-frequency air-frame vibration.

In presenting the results of the analysis of the data, it is not representative to consider either the maximum or minimum conditions. We have selected, purely arbitrarily, the median condition, wherein fifty per cent of the pictures will be taken under better conditions, fifty per cent under poorer conditions. One may argue with good justification that the value for the 90th percentile might be more in accord with practice—the practice wherein a large percentage of the photographs taken meet certain specifications. In our own case the median value seemed to work out well in comparative tests, and we have the feeling that the argument of the exact percentile at which the comparison is made is somewhat academic. In any case, as the analysis is made, one plots the frequency of occurrence of the image velocities and from this plot determines the value of image motion at the chosen percentile.

If the total motion effects are desired, we have described the analysis. If a mount comparison is desired, this also may be sufficient for complete analysis. In either case, it is desirable to record enough trails so that trails representative

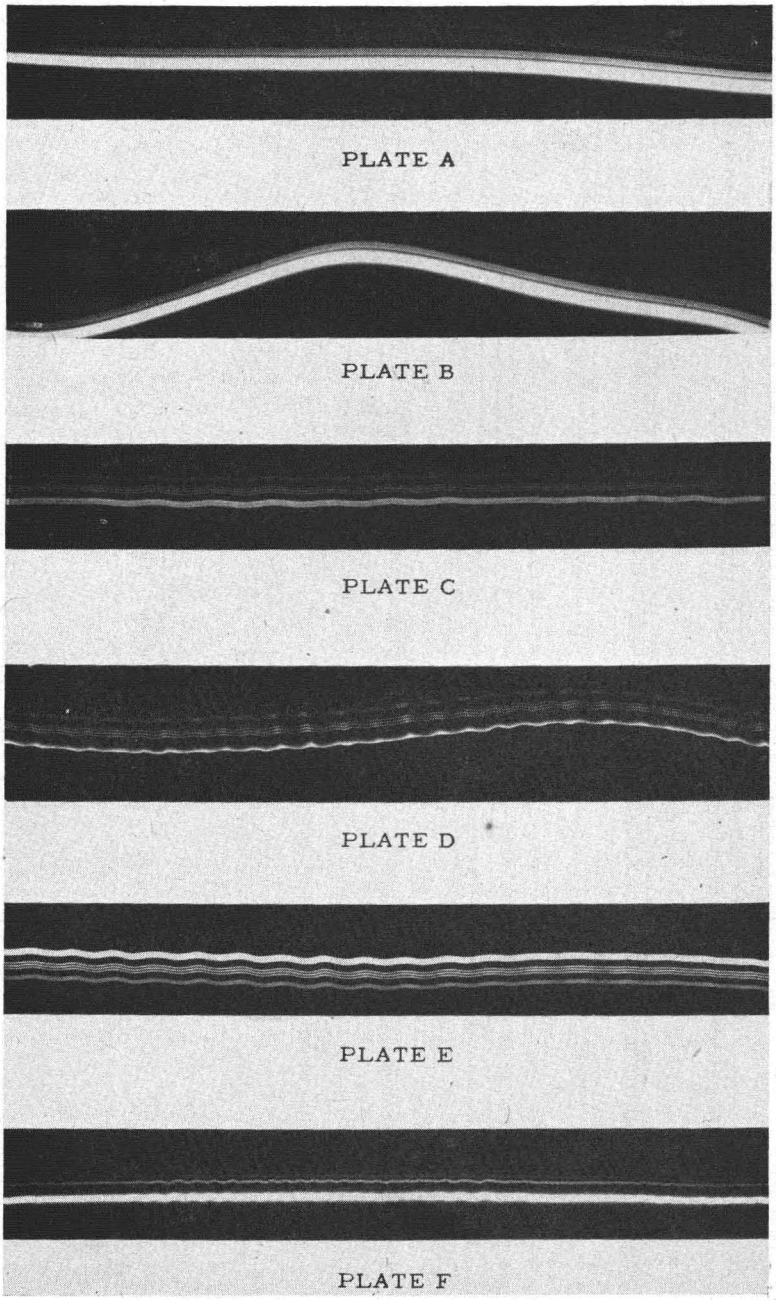

FIG. 4. Contact prints from vibration trails.

of typical aircraft motion be selected. If two mounts are compared on passes with similar (as judged by eye) aircraft motion, then the comparison is valid; if they are dissimilar, or if one desires the mount contribution alone, then it becomes necessary to subtract the aircraft motion effects. This is done in a manner illustrated in Figure 2, except, instead of using the raw data, we use the computed data. Representative amplitudes as computed are plotted on a graph as Figure 5. A smooth curve is then drawn through the points to represent the

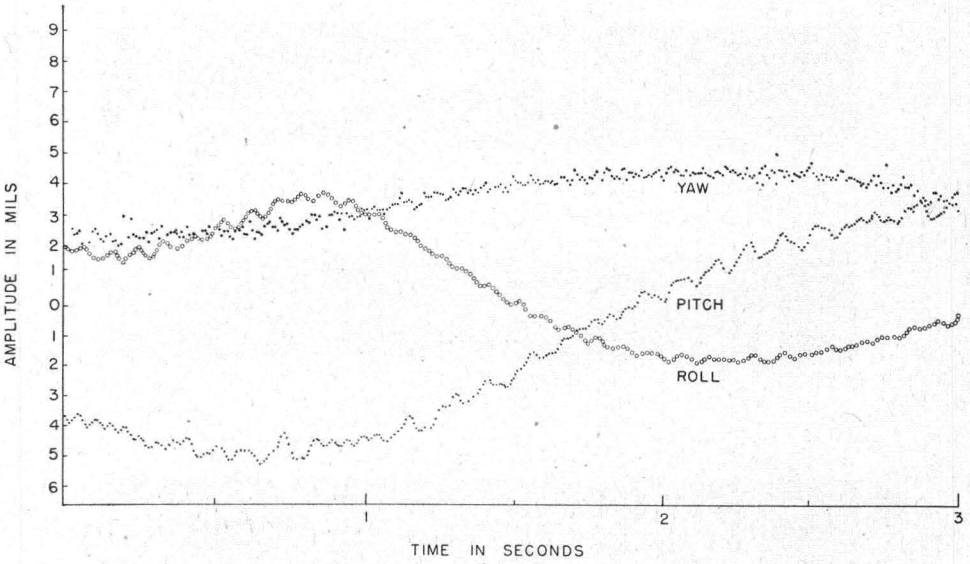

FIG. 5. Plot of the amplitudes of roll, pitch and yaw of a K-22 camera in the standard mount of an F-5E (flight record).

over-all aircraft motion. This curve is so drawn as to smooth out (i.e., eliminate) all motions of less than one second period. The aircraft motion at any point, as determined from this smoothed curve, must then be subtracted from the computed total motion; this leaves the motion due to the mount.

The aircraft motion for any point is given by the amplitude at that point minus the amplitude at the next point divided by the time interval between points, i.e., the change in amplitude divided by the time to make that change.

TABLE I. RATES OF AIRCRAFT MOTION

Mission	No. of Films	Av. Median Roll (mils./sec.)	Roll 90% of Time Less Than (mils./sec.)	No. of Films	Av. Median Pitch (mils./sec.)	Pitch 90% of Time Less Than (mils./sec.)
N-3	2	6.0	10.9	2	4.7	9.4
N-4	4	7.1	18.5	4	2.1	4.4
N-5	4	5.2	12.7	5	1.5	4.0
N-8	5	1.44	3.14	8	0.55	1.57
N-9	1	0.37	0.52	1	0.88	1.25
N-10	4	2.1	3.9	4	0.93	2.06
N-11	3	3.1	9.4	3	5.6	15.9
N-12	2	3.0	7.4	4	1.3	4.7

Again, this is read directly from the smoothed curve. As the total motion is made up of aircraft motion plus camera-mount motion, the camera-mount motion is, therefore, total motion as computed minus the aircraft motion as read from the smoothed curve.

Typical experimental results are tabulated in Tables I and II. Inasmuch as yaw was found negligible for the long focal length equipment tested, we have tabulated only roll and pitch data.

TABLE II. AVERAGE MEDIAN ANGULAR VELOCITIES IN MILS/SEC OF THE CAMERA-MOUNT SYSTEM

No. of Film	Mount	Lens	Camera	Roll	Pitch
6	A-11	24″	K-17	2.96	1.56
2	A-11PM*	24″	K-17	2.9	1.97
1	A-11BM*	24″	K-17	3.4	2.6
5	A-8	24″	K-17	1.79	1.51
2	A-27A	24″	K-17	4.2	4.6
2	East. Anti-Vib.†	24″	K-17	4.42	4.42
1	A-11	40″	K-22	1.88	1.66
1	A-11BM	40″	K-22	2.6	1.6
5	A-8	40″	K-22	2.75	2.79
7	East. Anti-Vib.	40″	K-22	4.02	3.00
4	c.g.	40″	K-22	0.99	0.67

* A-11 PM—Plywood modification. Plywood spacers replacing Lord Pads. A-11BM—Balsa modification. Balsa spacers replacing Lord Pads.

† Of the two Eastman Anti-Vibration mounts employed, one was equipped with heavy springs for the 40-inch camera, and the other with light springs for use with the 24-inch camera.

The combined magnitude of the accidental effects may be determined by dividing the phenomenon into effects in the line of flight and across the line of flight (yaw acting in both coordinates) and taking the root mean square of these values in each coordinate. Taking the most representative values we have today, we may tabulate for the 24-inch Aero Ektar at 10,000 feet, with 1/150 second exposure on Super-XX, the following factors (median values):

TABLE III. COMPARATIVE MAGNITUDE OF MOTION FACTORS IN 24-INCH PHOTOGRAPHY AT 10,000 FEET, SUPER-XX EMULSION, 1/150 SEC EXPOSURE, 200 MILES PER HOUR GROUND SPEED

	In Flight Line	Across Flight Line
Lens and film	0.040 mm.$^{-1}$	0.040 mm.$^{-1}$
Translation	0.119 mm.$^{-1}$	0.000 mm.$^{-1}$
Aircraft motion	0.008 mm.$^{-1}$ (pitch)	0.015 mm.$^{-1}$ (roll)
Camera-mount motion	0.011 mm.$^{-1}$ (pitch)	0.016 mm.$^{-1}$ (roll)
Yaw (mount plus aircraft)	0.001 mm.$^{-1}$	0.001 mm.$^{-1}$

We may then calculate performance. The RMS of the aircraft motion, camera-mount motion, and yaw in the line of flight is 0.0137 mm.$^{-1}$, and across the line of flight is 0.0221 mm.$^{-1}$. Thus, the image blur in the flight line is $0.040+0.119+0.014$, which is 0.173 mm.$^{-1}$ or its reciprocal, 5.8 lines/mm. Across the flight line this becomes $0.040+0.0221=0.062$ mm.$^{-1}$, or 16.1 lines/mm.

The calculation is in good agreement with flight tests based on an "heuristic" formula proposed by A. Katz,[3] namely, that the final resolution through a series

of degrading components is the reciprocal of the sum of the reciprocals of the individual resolutions, i.e.,

$$1/R_{a+b+c+\cdots} = 1/R_a + 1/R_b + 1/R_c + \cdots .$$

Although Schade[4] has recently refined this method, the results of the simple formula are good enough for general use. There is, in fact, a tinge of logic that can be applied to this approximation. Assume a lens gives 25-line/mm. resolution and a film also gives 25-line/mm. resolution. This means that the lens takes a point image and spreads it over a 1/25-mm. diameter blur (approximately). The film, by the same basis, takes each point in that 1/25-mm. blur of light and spreads it over a 1/25-mm. diameter (approximately) blur. The combined blur is, therefore, from this geometric consideration, 1/25+1/25, or 2/25 mm. (approximately).

A last note on image motion effects is illustrated by Figure 6. A geometric solution is presented for the case of the movement of a perfect line image across itself. It is seen that when the line has moved its own width, $\frac{1}{2}S$ (one-half the line+space width), the three line images are still imaged at full contrast; that only where the motion has been of the total length S does the contrast between line and space reduce to zero; and that at motions greater than S a form of geometric spurious resolution sets in, showing two lines in the image for the three-line object.

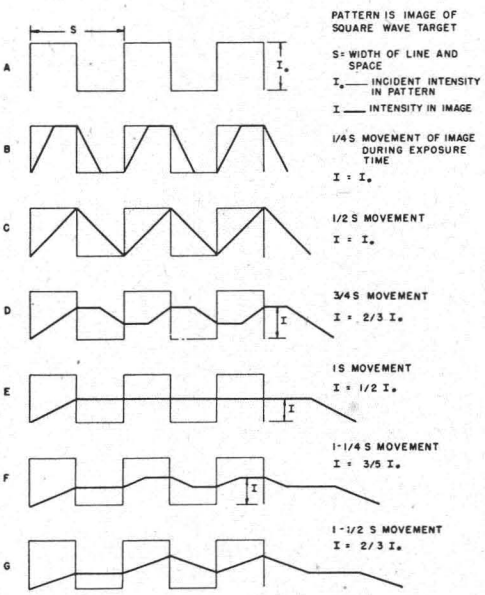

FIG. 6. Representation of the effect of image motion.

Mention should be made of attempts during the war to isolate ultra-high-frequency vibration components. A system was constructed to provide 20,000-cycle/sec. frequencies for the flashing light sources. The system consisted of a rotating cylinder a little over two feet in diameter with twenty 3×9-inch mirrors mounted on the periphery of this cylinder. The cylinder was illuminated by a collimated beam from a 1,000-cp. light source and rotated at speeds from 150 to 1,200 rpm. The flashes from this rotor were reflected along a row of fifty convex mirrors of about 70-inch radius of curvature, mounted at a 45-degree inclination to the line from the rotor to the line of mirrors. Thus, there were 20 flashes per rotation of the rotor times 50 flashes from each rotor flash from the convex mirrors.

Only a limited number of analyses were made from this maze of points, but there results, therefrom, good evidence that there is a considerable amplitude impressed in the roll-and-pitch curves at the instant of release of focal plane shutter, recoil velocities of the order of two mils per second, which subtract but a small fraction of the normal photographic exposure. Between-the-lens shut-

ters introduce much smaller effects, which are negligible compared to the motions subject to discussion in this paper.

Summary and Remarks

Experience gained from a few analyses, or even from the simple "inspection" method described in this paper, will enable rapid assessment of comparative system performance through the flashing light method. Inasmuch as roll effects are generally of the greatest magnitude of the accidental motions, and as our present experience has shown no air vehicle or camera-mount system giving results of different orders of magnitude in roll and pitch, the simple crude analysis made with common rule and by counting points is presented as a good approximation to the one coordinate (and therefore representative) performance.

We have considered that image movement in the focal plane is caused both by angular motion and translational motion. The dominant factor in most cases is translational motion. Image degradation due to these motion factors will exist even for exposures considerably shorter than those used in present-day aerial photography.

One first considers the possibility of having the mount participate in the compensation of image movement due to translation. This has been attempted: notably, the Chandler Mount. There is some indication, however, that when this mount is compensating for translation, its anti-vibration performance deteriorates (or, rather, the compensation itself sets up vibration). Other methods of compensation appear neater, easier, and in a less favorable position to impart vibration. It would appear that mounts should be designed only from the point of view of stability of the angular motions, and that image movement compensation should be attempted by other means not associated with the structure of the mount itself, e.g., film movement, rotating prisms, etc. This is consistent with the present direction of practice.

There are two types of angular motion impairing performance of aerial cameras:

(1) the motion of the aircraft as a whole, in general a low-frequency form of vibration;

(2) a high-frequency vibration of the camera in its mount.

These two effects are of about equal importance in the limitations they impose upon performance. To eliminate one and not consider the other does but half the job.

Camera stabilization systems are employed to remove the low frequencies, and are at present employed primarily in photogrammetric work. Anti-vibration systems are employed to remove the high-frequency vibrations, and are emphasized in reconnaissance work. Little emphasis has been placed on a combine. The longer focal lengths employed in reconnaissance do require anti-vibration systems, but no more so than they require stabilization. The ideal mount for reconnaissance cameras is a stabilized system of low natural frequency, high in compliance, not unlike a stabilized Chandler Mount, or better, a stabilized center-of-gravity system. It should be pointed out that vertical referencing is not important in this type of system and, therefore, the stabilization systems of the present day that are employed in mapping meet additional requirements which are not necessary for the reconnaissance problem.

These long-period aircraft motions may vary in amplitude over the aircraft, but they have been found at any given time to have the same frequencies over the aircraft. It would appear desirable to plot amplitudes over the aircraft, and

to select the photographic stations on the basis of findings from this type of study in addition to those from a study to determine the corresponding points of a minimum high-frequency vibration. These long period motions, which apparently vary somewhat from aircraft to aircraft, range in the order of from five to thirty cycles per minute. These are the motions that are treated through stabilization techniques.

It is perhaps possible, however, to eliminate this stabilization requirement for reconnaissance by development of a mount that would trip the shutter on the zero velocity point of the roll-amplitude curve of the aircraft, with a varying film speed to compensate for the pitch motion of the aircraft. The roll-and-pitch curves studied appear consistent enough over long periods to enable good prediction over short time intervals. The idea of a device that would activate the shutter only at the zero velocity point on the aircraft motion curves is not a solution to be overlooked. A method might be to employ a gyro recorder (predictor) of roll amplitudes, and a continuously moving film (i.e., moving film magazine) set to compensate for average translational image movement, with the platen that carries the film across the focal plane oscillating back and forth to introduce a $\pm\Delta V$ compensation for the pitch velocities. The shutter would then be set to trip only at maximum roll amplitudes. Such a solution involves control of small masses and thereby offers this advantage. Whether the system could react similarly to the higher-frequency vibrations would appear to be an open question.

In the past, too little attention has been paid to the advantage to be realized by supporting the camera system at the center of gravity. The trunnion position of the cameras should be located accurately at the center of gravity of the system (i.e., camera and attached portion of mount), and also should lie in the plane of the vibration dampers. A solution might be attained with adjustable masses to set the center of gravity to the trunnion plane for each lens cone employed with the camera, and to maintain a constant moment of inertia of the system.

Regarding the problem of a universal mount (taking loads of varying mass and mass distribution), a mount system might be considered that has provision for varying the dry-damping of the mount with the camera load. High-frequency vibrations proceed back and forth along the aircraft both in a longitudinal and lateral direction. To a first approximation, it can be said that the mount feet should be so spaced as to give equal stability in both directions. Because of the nature of the vibrations passing along the fuselage of the aircraft, it is possible that an irregular spacing of the mount feet along the longitudinal and transverse coordinates (e.g., in a trapezoid or parallelogram) would offer better support than the present mounting arrangement.

The encouraging results of vibration tests of the twin camera center-of-gravity mount, described in OSRD Report 6029, should be considered when undertaking a long-range development program for aerial camera mounts. This application should not be limited to two cameras. The possibility of mounting an entire battery of aerial cameras on a single center-of-gravity point support, with film winds opposed by matching one camera against another, offers the increased advantage of large mass. All experience with massive cameras indicates improved vibration characteristics. It may be argued that such mounts can come close to resonance with aircraft motions; however, with such systems it is possible to adjust the natural frequency of the entire mass, by careful balancing on the center of gravity, to a value lower than the frequency of the aircraft vibration which may go to the order of five cycles per minute. This system has

proven itself to be the best of the anti-vibration aerial camera mounts tested to date.

The high frequencies that are found in reciprocating engine aircraft are always about the same. Of course, engine beat frequencies may creep in through failure to synchronize the engines, but except for these the near constancy of the frequency is of interest. It apparently stems from the vibration of the airframe itself and has a fundamental of about 7 cps with a first harmonic, 14 cps, and sometimes the second harmonic, 28 cps, present. The fundamental is almost always within the range, 7 ± 1 cps. This is the prime high-frequency component that our anti-vibration mounts must combat.

In closing, we present for the record an idealized solution to aircraft roll, pitch, and yaw.*

Idealized Solution to Roll, Pitch and Yaw

Consider the path of a plane with uniform velocity and without yaw, pitch, or roll. Let the x axis be defined as the direction of flight, y as the altitude. Let AT = interval between flashes.

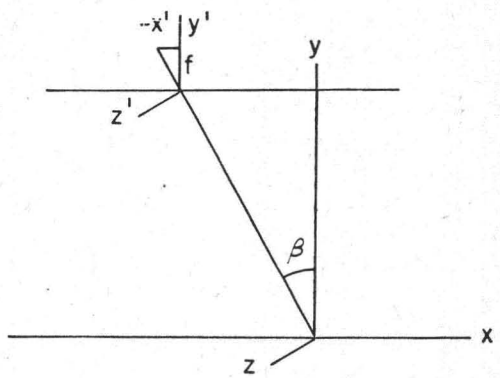

FIG. A

$$\frac{-x'}{f} = \tan\beta = \frac{-x}{y} \qquad \frac{dx}{dt} = v$$

$$\frac{+dx'}{f} = \sec^2\beta d\beta = \frac{+dx}{y} = \frac{vdt}{y}$$

$$\frac{dx'}{dt} = f\sec^2\beta\frac{d\beta}{dt} = \frac{vf}{y}. \qquad (1)$$

Now let y' be the upward normal from the center of film. Consider the plane in a random attitude with pitch ϕ, roll ψ, yaw θ. X' is in general direction of x but defined by the longitudinal axis of the plane.

Translate the primed axes so that the primed origin coincides with the unprimed. First both axes so that z is in the direction of z' and $\cos^{-1}(yy') = \phi$ also $\cos^{-1}(xx') = \phi$.

$$\begin{aligned} x &= x_1'\cos\phi + y_1'\sin\phi + z_1'[0] \\ y &= -x_1'\sin\phi + y_1'\cos\phi + z_1'[0] \\ z &= x_1'[0] + y_1'[0] + z_1'[1] \end{aligned} \qquad (2)$$

Let the radius of the sphere be unity.

(*See Fig. B on the next page*)

* This solution has been previously presented: see reference 5, pp. 622–636.

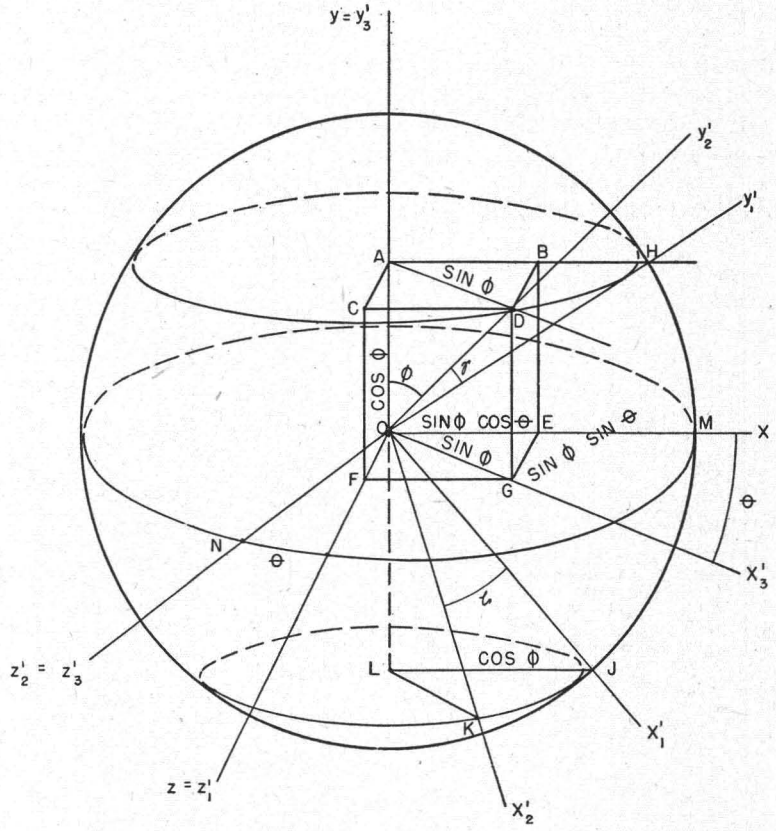

FIG. B

$$HD = 2 \sin \phi \sin \frac{\theta}{2}$$

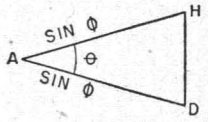

$$HD = 2 \sin \frac{\gamma}{2}$$

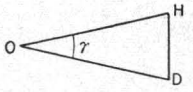

FIG. C

$$\sin \phi \sin \frac{\theta}{2} = \sin \frac{\gamma}{2}$$

$$\sin^2 \frac{\gamma}{2} = \frac{1 - \cos \gamma}{2}$$

$$\sin \phi \sin \frac{\theta}{2} = \sqrt{\frac{1 - \cos \gamma}{2}} \qquad \therefore \quad \frac{1 - \cos \gamma}{2} = \sin^2 \phi \sin^2 \frac{\theta}{2}$$

$$\cos\gamma = -2\sin^2\phi\sin\frac{\theta}{2} - 1$$

$$\sin\gamma = \sqrt{1 - \left(4\sin^4\phi\sin^4\frac{\theta}{2} - 4\sin^2\phi\sin^2\frac{\theta}{2} - 1\right)}$$

$$\sin\gamma = 2\sin\phi\sin\frac{\theta}{2}\sqrt{1 - \sin^2\phi\sin^2\frac{\theta}{2}}\,.$$

Rotate the system about y so that y_2' makes an angle with y_1' such that:

$$\cos\gamma = 1 - 2\sin^2\phi\sin^2\frac{\theta}{2} \quad \text{and}$$

$$\sin\gamma = 2\sin\phi\sin\frac{\theta}{2}\sqrt{1 - \sin^2\phi\sin^2\frac{\theta}{2}}\,.$$

Then

$$\begin{aligned} x_1' &= x_2'\left(1 - 2\cos^2\phi\sin^2\frac{\theta}{2}\right) - y_2'\sin\phi\cos\phi(1 - \cos\theta) \\ &\quad - z_2'\sin\theta\cos\phi \\ y_1' &= -x_2'\sin\phi\cos\phi(1 - \cos\theta) + y_2'\left(1 - 2\sin^2\theta\sin^2\frac{\theta}{2}\right) \\ &\quad - z_2'\sin\theta\sin\phi \\ z_1' &= x_2'\sin\theta\cos\phi - y_2'\sin\theta\sin\phi - z_2'\cos\theta \end{aligned} \tag{3}$$

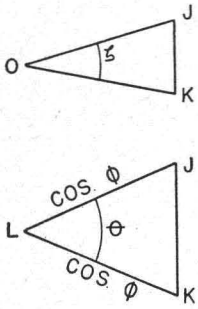

FIG. D

$$JK = 2\sin\frac{\zeta}{2} = 2\cos\phi\sin\frac{\theta}{2}$$

$$\sin\frac{\zeta}{2} = \cos\phi\sin\frac{\theta}{2}$$

$$\sin^2\frac{\zeta}{2} = \frac{1 - \cos\zeta}{2} = \cos^2\phi\sin^2\frac{\theta}{2}$$

$$1 - \cos\zeta = 2\cos^2\phi\sin^2\frac{\theta}{2}$$

$$\cos\zeta = \cos(x_1'x_2') = 1 - 2\cos^2\phi\sin^2\frac{\theta}{2}\,.$$

To find the angle between y_1' and y_2', solve the spherical right triangle HMN.

Known:

$$HM = \frac{\pi}{2} - \phi$$

$$MN = \frac{\pi}{2} + \theta$$

$$HMN = \frac{\pi}{2}$$

$$\cos HN = \cos (90 - \phi) \cos (90 + \theta) = - \sin \phi \sin \theta = \cos (y_1' z_2').$$

Now rotate the initial coordinate system about the y axis through an angle θ.

$$\begin{aligned} x &= x_3' \cos \theta + y_3'(0) - z_3' \sin \theta \\ y &= x_3'(0) + y_3'(1) + z_3'(0) \\ z &= x_3' \sin \theta + y_3'(0) + z_3' \cos \theta \end{aligned} \tag{4}$$

Next rotate about z through an angle ϕ,

$$\begin{aligned} x &= x_2' \cos \phi + y_2' \sin \phi + z_2'(0) \\ y &= - x_2' \sin \phi + y_2' \cos \phi + z_2'(0) \\ z &= x_2'(0) + y_2'(0) + z_2'(1) \end{aligned} \tag{5}$$

and substitute eqs. 5 into eqs. 4.

$$\begin{aligned} x &= x_2' \cos \theta \cos \phi + y_2' \cos \theta \sin \phi - z_2' \sin \theta \\ y &= - x_2' \sin \phi + y_2' \cos \phi + z_2'(0) \\ z &= x_2' \sin \theta \cos \phi + y_2' \sin \theta \sin \phi + z_2' \cos \theta. \end{aligned} \tag{6}$$

Equating eqs. 6 to eqs. 1 and rearranging,

$$\begin{aligned} x_1' &= x_2'(\cos \theta \cos^2 \phi + \sin^2 \phi) + y_2'[(\sin \phi \cos \phi)(\cos \theta - 1)] - z_2' \sin \theta \cos \phi \\ y_1' &= x_2'[(\sin \phi \cos \phi)(\cos \theta - 1)]\ y_2'(\cos \theta \sin^2 \phi + \cos^2 \phi) - z_2' \sin \theta \cos \phi \\ z_1' &= x_2' \sin \theta \cos \phi + y_2' \sin \theta \sin \phi + z_2' \cos \theta. \end{aligned} \tag{7}$$

We have now found all the angles involved in transforming from the xyz system with origin on the ground, (x = the direction of flight, y = upward vertical, z = horizontal to right) to x_2', y_2', z_2', in which the plane of the film is $x_2' z_2'$ with pitch ϕ positive with nose up, yaw θ positive to starboard. Roll has not yet been considered. Positive y_2' is in the direction of the optical axis away from lens.

Let the roll take place about x_2' axis through an angle counter clockwise as seen by an observer watching the plane approach him.

We then have as final axes attached to the film (x', y', z').

$$\begin{aligned} x_2' &= x'[1] + y'[0] + z'[0] \\ y_2' &= x'[0] + y' \cos \psi - z' \sin \psi \\ z_2' &= x'[0] + y' \sin \psi + z' \cos \psi \end{aligned} \tag{8}$$

$$\begin{aligned} x &= x' \cos \theta \cos \phi + y'(\cos \theta \sin \phi \cos \psi - \sin \theta \sin \psi) \\ &\quad - z'(\cos \theta \sin \phi \sin \psi + \sin \theta \cos \psi) \\ y &= - x' \sin \phi + y' \cos \phi \cos \psi - z'(\sin \theta \sin \phi \sin \psi - \cos \theta \cos \psi) \\ z &= x' \sin \theta \cos \phi + y'(\sin \theta \sin \phi \cos \psi + \cos \theta \sin \psi) \\ &\quad - z'(\sin \theta \sin \phi \sin \psi - \cos \theta \cos \psi) \end{aligned} \tag{9}$$

$$x' = x \cos \theta \cos \phi - y \sin \phi + z \sin \theta \cos \phi$$

$$
\begin{aligned}
y' &= x(\cos\theta \sin\phi \cos\psi - \sin\theta \sin\psi) + y \cos\phi \cos\psi \\
&\quad + z(\sin\theta \sin\phi \cos\psi + \cos\theta \sin\psi) \qquad (10) \\
z' &= -x(\cos\theta \sin\phi \sin\psi + \sin\theta \cos\psi) + y \cos\phi \sin\psi \\
&\quad + z(\sin\theta \sin\phi \sin\psi + \cos\theta \cos\psi).
\end{aligned}
$$

Now consider a set of axes x'', y'', z'', in which z'' is along the line of lights (to the right) $y''=y$. I.e. the course is not normal to the line of lamps but at an angle α to the normal.

Then

$$
\begin{aligned}
x &= x'' \cos\alpha + y''[0] + z'' \sin\alpha \\
y &= x''[0] + y''[1] + z''[0] \qquad (11) \\
z &= -x'' \sin\alpha + y''[0] + z'' \cos\alpha.
\end{aligned}
$$

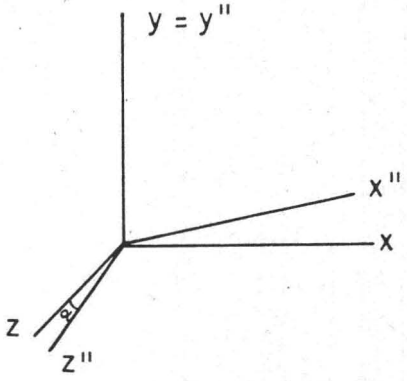

FIG. E

Substituting eqs. 11 into eqs. 10

$$
\begin{aligned}
x' &= x'' \cos(\alpha+\theta) \cos\phi - y'' \sin\phi + z'' \sin(\alpha+\theta) \cos\phi \\
y' &= x''[\cos(\alpha+\theta) \sin\phi \cos\psi - \sin(\alpha+\theta) \sin\psi] + y'' \cos\phi \cos\psi \\
&\quad + z''[\sin(\alpha+\theta) \sin\phi \cos\psi + \cos(\alpha+\theta) \sin\psi] \qquad (12) \\
z' &= -x''[\cos(\alpha+\theta) \sin\phi \sin\psi + \sin(\alpha+\theta) \cos\psi] + y'' \cos\phi \sin\psi \\
&\quad - z''[\sin(\alpha+\theta) \sin\phi \sin\psi - \cos(\alpha+\theta) \cos\psi].
\end{aligned}
$$

Next we must project a line parallel to z'' onto the plane of the film x', z', and express the two angles of the projection in terms of x' and z'. Then we must find the effect of β.

Let the lights be called A, B and C. Let B be at the origin of both the unprimed and doubly primed axes and BA in the direction of z''. Project AB upon a plane parallel to the $x'z'$ plane. The direction cosines of AB with $o'x'$, $o'y'$, and $o'z'$ respectively are:

$$
\begin{aligned}
&\sin(\alpha+\theta) \cos\phi; \\
&\sin(\alpha+\theta) \sin\phi \cos\psi + \cos(\alpha+\theta) \sin\psi; \\
&-\sin(\alpha+\theta) \sin\phi \sin\psi + \cos(\alpha+\theta) \cos\psi.
\end{aligned}
$$

Assuming sufficient depth of focus

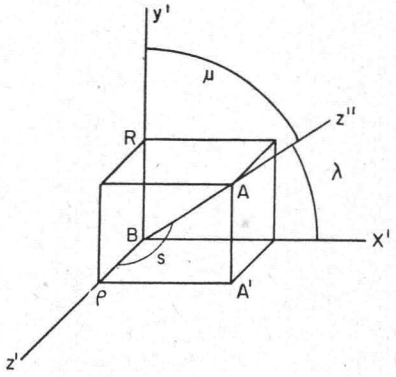

FIG. F

$z' \cos \mu = \cos (y'z'') = \sin (\alpha+\theta)$

$\sin \mu = \sin (yz'')$

$$= \sqrt{1-\sin^2(\alpha+\theta)\sin^2\phi\cos^2\psi - [2\sin(\alpha+\theta)\cos(\alpha+\theta)][\sin\phi\sin\psi\cos\psi] - \cos^2(\alpha+\theta)\sin^2\psi}$$

$BA' \sin \mu \cos PBA' = BP$

$$\frac{BP}{BA} = \cos\nu = \cos(\alpha+\theta)\cos\psi - \sin(\alpha+\theta)\sin\phi\sin\psi = \sin\mu\cos PBA'$$

$$\therefore \cos PBA' = \frac{\cos(\alpha+\theta)\cos\psi - \sin(\alpha+\theta)\sin\phi\sin\psi}{\sqrt{1-\sin^2(\alpha+\theta)\sin^2\phi\cos^2\psi - 2\sin(\alpha+\theta)\cos(\alpha+\theta)\sin\phi\sin\psi\cos\psi - \cos^2(\alpha+\theta)\sin^2\psi}}$$

$BQ = BA \sin \mu \cos QBA'$

$$\frac{BQ}{BA} = \cos\lambda = \sin(\alpha+\theta)\cos\phi = \sin\mu\cos(QBA')$$

$$\therefore \cos(QBA') = \frac{\sin(\alpha+\theta)\cos\phi}{\sqrt{1-\sin^2(\alpha+\theta)\sin^2\phi\cos^2\psi - 2\sin(\alpha+\theta)\cos(\alpha+\theta)\sin\phi\sin\psi\cos\psi - \cos^2(\alpha+\theta)\sin^2\psi}}$$

$\cos RBA' = 0.$

Thus, we have the three direction cosines of $B'A'$ (The projection of BA) with $o'x'$, $o'y'$, and $o'z'$. This means that on the center of the film we can express the sine of the angle between z' and $B'C'$ as $\sqrt{1-\cos^2(PBA')}$ since the image is reversed on the film.

Looking down on the film from above the camera (See Fig. G)

$$\sin\rho = \frac{\sin(\alpha+\theta)\cos\phi}{\sqrt{1-\sin^2(\alpha+\theta)\sin^2\phi\cos^2\psi - 2\sin(\alpha+\theta)\cos(\alpha+\theta)\sin\phi\sin\psi\cos\psi - \cos^2(\alpha+\theta)\sin^2\psi}}.$$

Now introduce the angle β which is the angle at the ground (center light, B) between the vertical and the line connecting B with the airplane.

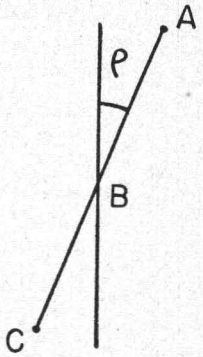

FIG. G

Consider two images of lamp B with a time interval t separating them. Call these B_1', and B_2' separated by time $t_2 - t_1 = t$.

Let the velocity of the aircraft $= v$ in the direction of x.

Let the elevation of the plane $= h$.

Let the focal length of the lens $= f$.

Let $f/h = r$

Then $\overline{B'A'}$ equals $r\overline{BA}$ for all values of β when θ, α, ϕ and ψ equal 0. $\overline{B'A'} = r\overline{BA} = \sin \mu$

$$\overline{B'A'}=r\overline{BA}\sqrt{1-\sin^2(\alpha+\theta)\sin^2\phi\cos^2\psi-2\sin(\alpha+\theta)\cos(\alpha+\theta)\sin\phi\sin\psi\cos\psi-\cos^2(\alpha+\theta)\sin^2\psi}$$

for all values of β

We can now tabulate the values of $\overline{B'A'}$ the restrictions listed.

BA'	β	α	θ	ϕ	ψ
$r\overline{BA}\cos\psi$	all values	0	0	all values	—
$r\overline{BA}\sqrt{1-\cos^2(\alpha+\theta)\sin^2\psi}$	all values	—	—	0	—
$r\overline{BA}\sqrt{1-\sin^2(\alpha+\theta)\sin^2\psi}$	all values	—	—	—	0
$r\overline{BA}$	all values	all values	all values	0	0

Rotate the unprimed axes about the z axis through an angle β such that $\tan\beta=vt/h$, $t=0$ when the airplane is directly overhead. As the airplane travels along parallel to the x axis taking a picture of lamp B every ΔT seconds, it is the same as if the airplane took one shot at a row of lights along the x axis spaced $v\Delta t$ feet apart. We therefore want a projection on the $x'z'$ plane (plane of the film) of a vector $\overline{BB_1}$, from B to B_1 (a distance of $v\Delta t$ feet). This projection will be of $\overline{BB_1}\cos\beta$ (in the direction of the x axis).

We must therefore rotate XYZ about the z axis through an angle β.

$$\begin{aligned}
\beta &= \tan^{-1}\frac{vt}{h}\\
x &= x_2\cos\beta + y_2\sin\beta + z_2(0)\\
y &= -x_2\sin\beta + y_2\cos\beta + z_2(0)\\
z &= x_2(0) + y_2(0) + z_2(1).
\end{aligned} \tag{13}$$

Equating the values of XYZ, of eq. 13 to these of eq. 9

$$\begin{aligned}
x_2 &= x'(\cos\beta\cos\theta\cos\phi + \sin\beta\sin\phi)\\
&\quad + y'(\cos\beta\cos\theta\sin\phi\cos\psi - \sin\beta\cos\phi\cos\psi - \cos\beta\sin\theta\sin\psi)\\
&\quad + z'(-\cos\beta\cos\theta\sin\phi\sin\psi - \cos\beta\sin\theta\cos\psi + \sin\beta\cos\phi\sin\psi)\\
y_2 &= x'(\sin\beta\cos\theta\cos\phi - \cos\beta\sin\phi)\\
&\quad + y'(\sin\beta\cos\theta\sin\phi\sin\psi + \cos\beta\cos\phi\cos\psi - \sin\beta\sin\theta\sin\psi)\\
&\quad + z'(-\sin\beta\cos\theta\sin\phi\sin\psi - \sin\beta\sin\theta\cos\psi - \cos\beta\cos\phi\sin\psi)\\
z_2 &= x'(\sin\theta\cos\phi) + y'(\sin\theta\sin\phi\cos\psi + \cos\theta\sin\psi)\\
&\quad - z'(\sin\theta\sin\phi\sin\psi - \cos\theta\cos\psi).
\end{aligned} \tag{14}$$

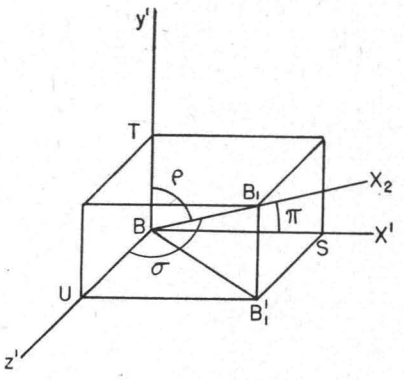

FIG. H

Now project X_2, that is BB' on the $x'z'$ plane. This projection is

$$BB_1' = BB_1 \sin \rho$$

$$\cos \rho = \cos y_1' x_2$$

$$\cos \rho = \cos \beta \cos \theta \sin \phi \cos \psi - \sin \beta \cos \phi \cos \psi - \cos \beta \sin \theta \sin \psi$$

$$\sin \rho = \sqrt{1 - \cos^2 \rho}$$

$$BB_1 \sin \rho \cos (U, \overline{BB_1}') = BU = BB_1 \cos \sigma = BB_1 \cos (z', x_2)$$

$$\therefore \quad \cos (U, BB_1') = \frac{1}{\sin \rho} (- \cos \beta \cos \theta \sin \phi \sin \psi - \cos \beta \sin \theta \cos \psi + \sin \beta \cos \phi \sin \psi)$$

$$BB_1 \sin \rho \cos (S, BB_1') = BS = BB_1 \cos \pi = BB_1 \cos (x_1' x_2)$$

$$\therefore \quad \cos (S, BB_1') = \frac{1}{\sin \rho} (\cos \beta \cos \theta \cos \phi + \sin \beta \sin \phi)$$

$$\cos T, \overline{BB_1}' = 0.$$

Thus we have the three direction cosines of BB_1' (The projection of BB_1) with $O'X'$, $O'Y'$ and $O'Z'$.

Summarizing, we wish to find

$$\theta = f_1(t)$$

$$\phi = f_2(t)$$

$$\psi = f_3(t)$$

We have the following variables:

Known	Unknown
Δt	v
h	α
f	β
$\overline{AB}$	θ
$\overline{BC}$	ϕ
	ψ

$\overline{B_0 B_1} = v\Delta t$

First find v by measuring a portion of the trail along the x axis, $v = \bar{x}/nr\Delta t$ where $\overline{X}$ is the length of the trail, n the number of points and $r = f/h$.

$\beta = f(t)$ and to a first approximation $\tan \beta = X/f$.

Then looking up from the lens

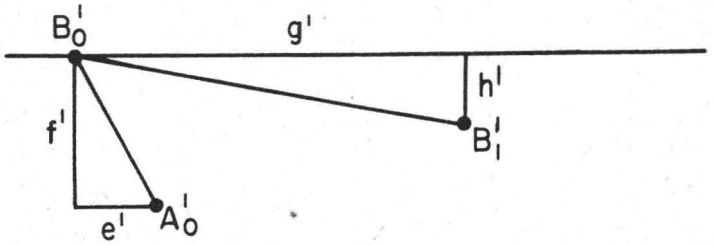

FIG. I

The projection of BA is

$$B_0'A_0' = r\overline{BA}(1 - \sin^2(\alpha+\theta)\sin^2\phi\cos^2\psi - \cos^2(\alpha+\theta)\sin^2\psi - 2\sin(\alpha+\theta)\cos(\alpha+\theta)\sin\phi\sin\psi\cos\psi)^{1/2}.$$

The X'-projection of this is

$$r\overline{BA}\sin(\alpha+\theta)\cos\phi \tag{15}$$

The Z'-projection of this is

$$r\overline{BA}[\cos(\alpha+\theta)\cos\psi - \sin(\alpha+\theta)\sin\phi\sin\psi]. \tag{16}$$

The projection of BB_1 is

$$B_0'B_1' = rB_0B_1[1 - \cos\beta\cos\theta\sin\phi\sin\psi - \sin\beta\cos\phi\cos\psi - \cos\beta\sin\theta\sin\psi)^2]^{1/2}.$$

The X projection of this is

$$r\overline{B_0B_1}(\cos\beta\cos\theta\cos\phi + \sin\beta\sin\phi). \tag{17}$$

The Y projection of this is

$$r\overline{B_0B_1}(-\cos\beta\sin\theta\cos\psi - \cos\beta\cos\theta\sin\phi\sin\psi + \sin\beta\cos\phi\sin\psi).$$

This gives 4 equations to solve for the four unknowns α, θ, ϕ and ψ.

$$\begin{aligned} e' &= r\overline{BA}\sin(\alpha+\theta)\cos\phi \\ f' &= r\overline{BA}[\cos(\alpha+\theta)\cos\psi - \sin(\alpha+\theta)\sin\phi\sin\psi] \\ g' &= r\overline{B_0B_1}(\cos\beta\cos\theta\cos\phi + \sin\beta\sin\phi) \\ h' &= r\overline{B_0B_1}(-\cos\beta\sin\theta\cos\psi - \cos\beta\cos\theta\sin\phi\sin\psi + \sin\beta\cos\phi\sin\psi) \end{aligned} \tag{18}$$

Let

$$\frac{e'}{r\overline{BA}} = e, \quad \frac{f'}{r\overline{BA}} = f, \quad \frac{g'}{rB_0B_1} = g \quad \text{and} \quad \frac{h'}{rB_0B_1} = h,$$

Then the four equations can be written:

$$\begin{aligned} e &= \sin\alpha\cos\theta\cos\phi + \cos\alpha\sin\theta\cos\phi \\ d &= \cos\alpha\cos\theta\cos\psi - \sin\alpha\sin\theta\cos\psi - \sin\alpha\cos\theta\sin\phi\sin\psi \\ &\quad - \cos\alpha\sin\theta\sin\phi\sin\psi \\ g &= \cos\beta\cos\theta\cos\phi + \sin\beta\sin\phi \end{aligned} \tag{19}$$

$$h = -\cos\beta \sin\theta \cos\psi - \cos\beta \cos\theta \sin\phi \sin\psi + \sin\beta \cos\phi \sin\psi.$$

The exact solution involves an equation of degree 36. Thus it is deemed advisable to assume that the unknown angles are small.

We then write

$$\sin x = x$$

$$\cos x = 1 - \frac{x^2}{2}$$

and neglect terms of third degree and higher.

Let

$$(\alpha + \theta) = \omega$$

$$e = \sin\omega \cos\phi$$

$$f = \cos\omega \cos\psi - \sin\omega \sin\phi \sin\psi$$

etc.

Then

$$e = \omega\left(1 - \frac{\phi^2}{2}\right) = \omega \tag{20}$$

$$f = \left(1 - \frac{\omega^2}{2}\right)\left(1 - \frac{\psi^2}{2}\right) - \omega\phi\psi = 1 - \frac{\omega^2}{2} - \frac{\psi^2}{2} \tag{21}$$

$$g = \cos\beta\left(1 - \frac{\theta^2}{2}\right)\left(1 - \frac{\phi^2}{2}\right) + \sin\beta(\psi)$$

$$= \cos\beta - \cos\beta\left(\frac{\theta^2}{2} + \frac{\phi^2}{2}\right) + \psi \sin\beta \tag{22}$$

$$h = -\cos\beta(\theta)(\psi) - \cos\beta\left(1 - \frac{\theta^2}{2}\right)\phi\psi + \sin\beta\left(1 - \frac{\phi^2}{2}\right)\psi$$

$$= -\cos\beta(\theta\psi + \phi\psi) + \psi \sin\beta. \tag{23}$$

Solving:

$$\omega = e \quad \text{from [21]}$$

$$\frac{\psi^2}{2} = 1 - \frac{\omega^2}{2} - f \quad \text{from [22]}$$

$$\psi = \pm\sqrt{2 - 2f - e^2}$$

from [23]

$$g = \cos\beta\left(1 - \frac{\theta^2}{2} - \frac{\phi^2}{2}\right) \pm \sqrt{2 - 2f - e^2}\sin\beta$$

$$g \sec\beta \pm \sqrt{2 - 2f - e^2}\tan\beta - 1 = -\frac{\theta^2}{2} - \frac{\phi^2}{2}$$

$$\theta^2 + \phi^2 = 2\left[1 - g \sec\beta \pm \sqrt{2 - 2f - e^2}\tan\beta\right] = N \tag{24}$$

from

$$h = \mp \theta\sqrt{2 - 2f - e^2}\cos\beta \mp \phi\sqrt{2 - 2f - e^2}\cos\beta \pm \sqrt{2 - 2f - e^2}\sin\beta$$

$$\theta + \phi = \tan\beta \mp \frac{h\sec\beta}{\sqrt{2 - 2f - e^2}} = M$$

$$\theta^2 + \phi^2 = N$$

$$\theta + \phi = M$$

$$M^2 - 2M\phi + 2\phi^2 = N, \qquad 4\phi^2 - 4M\phi + M^2 = 2N - M^2$$

$$2\phi - M = \pm\sqrt{2N - M^2}$$

$$\phi = \tfrac{1}{2}[M \pm \sqrt{2N - M^2}], \qquad \theta = \tfrac{1}{2}[M \mp \sqrt{2N - M^2}]$$

$$\alpha = \omega - \theta.$$

Thus we write the solution:

$$\alpha = e - \tfrac{1}{2}[M \mp \sqrt{2N - M^2}]$$

$$\theta = \tfrac{1}{2}[M \mp \sqrt{2N - M^2}]$$

$$\phi = \tfrac{1}{2}[M \pm \sqrt{2N - M^2}]$$

$$\psi = \pm\sqrt{2 - 2f - e^2}$$

where

$$M = \tan\beta \mp \frac{h\sec\beta}{\sqrt{2 - 2f - e^2}}$$

$$N = 2[1 - g\sec\beta \pm \tan\beta\sqrt{2 - 2f - e^2}]$$

Acknowledgments

For the most part, this paper describes work performed at the Massachusetts Institute of Technology and at Harvard University, during World War II. All those associated with these projects contributed freely and helpfully to this program. The data have been freely taken from two wartime reports, so much so that no detailed reference was felt possible. These reports are listed as references 2 and 5, and serve as general background. In particular, one must acknowledge the contributions of Miss Lillian R. Elveback, Miss Ruth Potter, Dr. R. M. Frye, Mr. Harold Zeoli, and the USAF pilots involved in the many flight tests, as well as the contributions of time and assistance of the personnel of the Wright Field Photo Reconnaissance Laboratory.

References

1. Mount Wilson Observatory Staff, Resolving Power in Aerial Photography (*OSRD Report* No. 4047, 1945). Contractor: Mount Wilson Observatory.
2. Macdonald, D. E., Progress Report on Aerial Camera Motions (*OSRD Report* No. 5178, June 1945). Contractor: Massachusetts Institute of Technology.
3. Katz, A. H., "Camera Shutters," *J. Opt. Soc. Am. 39*, 1–21 (1949).
4. Schade, O. H., "Electro-Optical Characteristics of Television Systems" (in four parts), *RCA Review 9*, 5–37, 245–286, 490–530, 653–686 (1948).
5. Macdonald, D. E., Quantitative Studies and Observations of Factors Limiting Resolution in Aerial Photography: Vol. I, Flight Data and Test Equipment; Vol. II, Analysis of Data, Conclusions and Recommendations; Vol. III, Appendix (*OSRD Report* No. 6029, December 1945). Contractor: Harvard University Optical Research Laboratory.